EXACT SOLUTION OF THE YOUNAN-VELETSOS PROBLEM

A NON-PEER-REVIEWED PREPRINT UPLOADED TO ENGRXIV

Joaquin Garcia-Suarez
Graduate Aerospace Laboratories
California Institute of Technology
California, CA 91125
ajgarcia@caltech.edu

Domniki Asimaki
Mechanical and Civil Engineering
California Institute of Technology
California, CA 91125
asimaki@caltech.edu

November 20, 2019

ABSTRACT

The assessment of forces exerted by the soil over walls is a recurrent problem in Geotechnical Engineering, owing to its relevance for both retaining systems and underground structures. In particular, the work by Veletsos and Younan becomes pertinent when it comes to consider pressure increments on underground structures triggered by seismic events. These scholars furnished the first satisfactory engineering solution corresponding to a simple configuration, which has become a milestone in the field. The exact solution to this reference problem is provided in the text. The solution is given in horizontal wavenumber domain, hence it comes in terms of inverse Fourier transforms, what entails not impediment for its numerical evaluation and verification against finite-element simulations.

***K*eywords** Geotechnical Engineering · Retaining Walls · Elastodynamics · Mathematical Modelling

1 Introduction

The study of the forces that soil exerts over retaining structures dates back centuries. A first clear distinction can be made, based on the methods used for the study:

- Methods based on plastic behavior of soils, foremost, limit-state theory [Lubliner, 2008], for so-called *yielding* walls, that is, walls that move enough as to elicit plastic response in the soil.
- Those that use the theory of Linear Elasticity to describe both soil and structure [Love, 2013], which presupposes small deformation in both soil and wall, and thus the wall in this case is termed *unyielding*.

The proper approach for the analysis does depend on the typology of the wall that is to be assessed or designed. Static load scenarios can be designed following the classic methods [Coulomb, 1973]; on the contrary, when it comes to considerations in the dynamic earthquake setting, the right path remains unclear to this day.

On one hand, yielding walls require to consider the soil plastic behavior, what is rather complicated in time-domain, and thus researchers have proposed *pseudo-static* methods, that, in spite of intrinsic limitations, deliver satisfactory, even conservative, outcomes for free-standing gravity or cantilever walls (except if resting on stiff rock). On the other hand, approaches based on Linear Elasticity are suitable to ascertain seismic pressures on unyielding walls (as, e.g., restrained basement walls or rigid-enough underground structures), as long as the structure whose walls are being analyzed does not experiment other soil-structure interaction (SSI) effects (rocking). The National Earthquake Hazard Reduction Program (NEHRP) recommendations [Building Seismic Safety Council, 2009] sanction this classification, while also suggests that a wall whose top deflects around 0.002 times its height already triggers plastic behavior in its soil vicinity, ergo the threshold to consider a wall as yielding is in practice fairly narrow.

The influence of soil-structure interaction, the effect of water in the backfill, the role of soil cohesion on the seismic response, as well as other topics, are still a matter of ongoing study.

1.1 Approaches based on Limit-state Theory

Pertaining to the first group, the forerunner is the classic method devised by Coulomb [Coulomb, 1973], under the tenets of what nowadays is called limit-state theory [Lubliner, 2008]. This method was developed to describe the response of yielding walls (sliding or rotating) under the action of its own weight and the one of the soil in the backfill. Its adaptation, for cohesionless soils, to attempt to consider also accelerations due to earthquakes came after the great Kanto earthquake (1923), which devastated a number of retaining walls (in paticular, the quay walls of the harbor of Yokohama), and it is referred to as the Mononobe-Okabe (M-O) Method [Okabe, 1924].

A number of similar improved schemes were developed later [Seed, 1970, Steedman and Zeng, 1990], leading to the a state-of-the-art model by Mylonakis and collaborators [Mylonakis et al., 2007].

All these methods framed the problem in a pseudo-static setting, wherein the earthquake load boils down to another acceleration to consider concurrently with gravity. One can acknowledge the inherent limitations of such approaches:

- They assume that the wall has already deformed outward (away from the soil) so as to generate an active earth pressure, and assume an active triangle soil wedge running from the base of the retaining wall to the surface.
- The soil behind the wall behaves as a rigid body, so accelerations are uniform at the interface between wall and soil, and thus they ignore wave propagation phenomena and their oscillatory nature, being thus unable to provide the actual distribution of pressures, just an estimate of the resultant force. This issue is the more apparent the taller the wall.
- Finally, it is impossible accommodate wall flexibility locally into the framework: either the wall moves as a rigid body or it remains completely still.

Moreover, there is a lack of consensus both on how to define the earthquake acceleration that is to added to gravity and how to consider heterogeneous backfills. In spite of these issues, these methods enjoy wide use to this day and seem to provide satisfactory design up to PGA 0.4 g [Candia et al., 2016].

1.2 Approaches based on Elasticity

When straining of both the soil and wall remains relatively small, Linear Elasticity theory provides a proper framework to describe its evolution. The only completely rigorous solution (from the mathematical standpoint) using this approach was obtained by Wood [Wood, 1973]. He considered a 2D finite stratum of soil on rigid bedrock confined between walls deforming under linear-elastic plane-strain conditions. In spite that this configuration may resemble a different system at first, logic dictates that if the distance between walls increases, the effects of a wall over the other one must fade, leaving the system virtually equivalent to the one-wall configuration insofar the displacement field around the wall is concerned. Hence, the problem may well be dubbed the *singular* Wood's problem. Nevertheless, his solution's mathematical "decorum" is overshadowed by being unintuitive (the mathematical expressions do not lend themselves to straightforward physical interpretation), in particular when the distance between walls tend to infinity, and also troublesome to evaluate numerically.

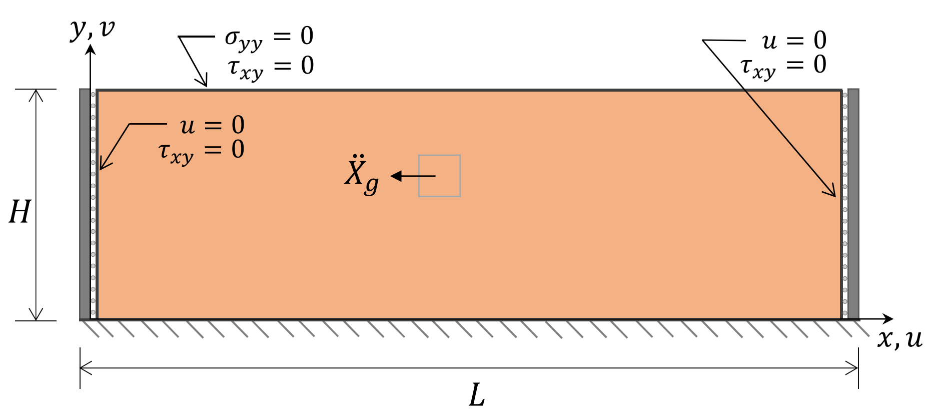

Figure 1: System solved by Wood (1973)

Simplified models for one-wall systems have been developed throughout the years in order to circumvent this issue, but every effort of tackling this very problem relied on introducing some sort of simplification. A number of them relied on either proposing a kind of, what, following Verruijt [Verruijt, 1996], one may refer as *confined* elastodynamic solutions, wherein a displacement component. Examples of the first have been successfully implemented in elastostatics [Westergaard, 1938] and elastodynamics [Barends, 1980].

The first attempt to consider a one-wall system directly trace back to the work by Matsuo and Ohara [Matsuo and Ohara, 1960]. They assumed a *confined solution* in which no vertical displacement develops anywhere in the soil domain, not even at regions close to the wall. This solution happened to be unbounded in the incompressible-material limit (undrained soil conditions).

The classic solutions for the one-wall case are due to Veletsos and Younan [Veletsos and Younan, 1994b, Veletsos and Younan, 1994a]. In the first, a variation of the confined solution was utilized: instead of neglecting a component of the displacement field, these researchers assumed that no normal vertical stress develops anywhere in the soil ($\sigma_{yy} = 0$ everywhere) in order to simplify and subsequently solve the equations of motion, so a solution for the displacement field, over the whole domain, could be retrieved. Regrettably, satisfying vertical equilibrium and the boundary condition $\tau_{xy}|_w = 0$ became impossible due to the introduction of this severe simplification.
In the second, [Veletsos and Younan, 1994b], a substantial improvement on Scott's model [Scott, 1973] was presented. It was assumed that the soil stratum behaves as an elastically-supported, semi-infinite horizontal viscoelastic bar with distributed mass and that the horizontal gradient of vertical displacements in the calculation of shear stresses is negligible, and thus a solution for the medium impedance was derived, so the stress field on the wall can be related to the simpler displacement field in the far-field (referred as "1D soil column" or "shear beam").
Later [Younan and Veletsos, 2000], their analysis was refined to consider different wall typologies, yet the foregoing simplifications were kept. Nevertheless, this work became the first one in attempting to include the effect on wall flexibility on the magnitude and distribution of pressures.

State-of-the-art models, as those proposed by Kloukinas and collaborators [Kloukinas et al., 2012], later used in the already-mentioned "kinematic framework" [Brandenberg et al., 2015], have been directly influenced by the Veletsos-Younan landmark work, and inherit the same pivotal assumption.

A more detailed summary of these and other previous studies can be found in a recent paper provided by [Keykhosropour and Lemnitzer, 2019].

At last, one must also highlight that problems in Elastic Waveguide Theory [Miklowitz, 2012] resemble the problem at hand, the solution of wave propagation in plates in plane stress being very mathematically similar the object of this manuscript, and thus it does not come as a surprise that solution techniques in this area can be also used for this problem.

2 Derivation of the exact solution in horizontal wave-number domain

The system is conformed by a rigid wall which is connected to rigid base (bedrock) and restrains a layer of soil. No specific boundary conditions, other than rigidity, were used for the wall in Veletsos and Younan original work, as the simplifying constraint they introduced, $\sigma_{yy} = 0$, precluded these consideration anyway. Following Wood [Wood, 1973], we shall consider that the wall is *smooth*, i.e., frictionless, and thus no shear stress develops the interface.

2.1 Presentation: total displacements

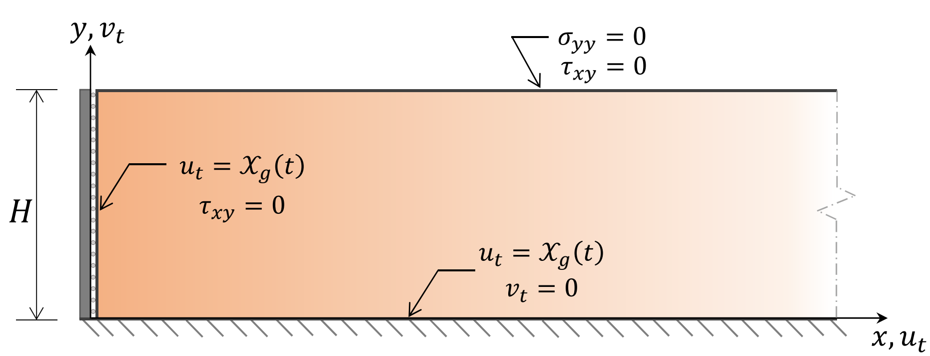

Figure 2: System framed in terms of total displacements

Consider an semi-infinite soft-soil layer, resting on rigid bedrock and bounded to the left by a rigid (thus it moves with the bedrock base) and smooth (thus no shear stresses develop at the soil-wall interface) wall.

The excitation of the system is an imposed time-varying displacement at the base $\mathcal{X}_g(t)$, which is supposed to be known and which cannot be affected by waves propagatin in the soil bulk.

Assuming that the soil behaves as a homogeneous, density ρ, isotropic linear-elastic solid (characterized by Lamé parameters μ, shear modulus, and λ), undergoing small deformations, the equations that govern the material dynamic response are the so-called Cauchy-Navier equations [Verruijt, 1996]:

$$(\lambda+2\mu)\frac{\partial^2 u_t}{\partial x^2}+(\lambda+\mu)\frac{\partial^2 v_t}{\partial x\partial y}+\mu\frac{\partial^2 u_t}{\partial y^2}=\rho\frac{\partial^2 u_t}{\partial t^2}\,, \tag{1a}$$

$$(\lambda+2\mu)\frac{\partial^2 v_t}{\partial y^2}+(\lambda+\mu)\frac{\partial^2 u_t}{\partial x\partial y}+\mu\frac{\partial^2 v_t}{\partial x^2}=\rho\frac{\partial^2 v_t}{\partial t^2}\,, \tag{1b}$$

subjected to the following boundary conditions: At $y=0$

$$u_t(x,y=0,t)=\mathcal{X}_g(t) \qquad v_t(x,y=0,t)=0\,, \tag{2a}$$

and at $y=H$

$$\tau_{xy}(x,y=H,t)=0 \qquad \sigma_{yy}(x,y=H,t)=0\,, \tag{2b}$$

and at $x=0$

$$\tau_{xy}(x=0,y,t)=0 \qquad u_t(x=0,y,t)=\mathcal{X}_g(t)\,. \tag{2c}$$

Hysteretic damping to the material can be achieved by simple substitution of the real shear modulus μ by $\mu(1+\mathrm{i}\delta_d)$, where δ_d can be referred as "loss factor".

2.2 Introduction of relative displacements

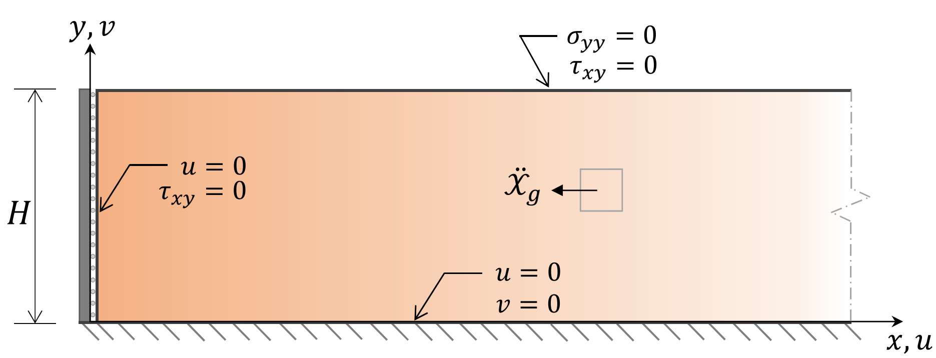

Figure 3: System re-framed in terms of relative displacements

Both u_t and v_t represent total displacements, measured with respect to some unmoved reference. For this particular problem, it turned out to be very useful to work with relative displacements instead. Thus, the change of variable $u_t(x,y,t)=u(x,y,t)+\mathcal{X}_g(t)$, $v_t(x,y,t)=v(x,y,t)$ is introduced in eq. (1) to obtain the equations of motion in terms of relative displacements

$$(\lambda+2\mu)\frac{\partial^2 u}{\partial x^2}+(\lambda+\mu)\frac{\partial^2 v}{\partial x\partial y}+\mu\frac{\partial^2 u}{\partial y^2}=\rho\frac{\partial^2 u}{\partial t^2}+\rho\ddot{\mathcal{X}}_g(t)\,, \tag{3a}$$

$$(\lambda+2\mu)\frac{\partial^2 v}{\partial y^2}+(\lambda+\mu)\frac{\partial^2 u}{\partial x\partial y}+\mu\frac{\partial^2 v}{\partial x^2}=\rho\frac{\partial^2 v}{\partial t^2}\,, \tag{3b}$$

as for eq. (2a):

$$u(x,y=0,t)=0 \qquad v(x,y=0,t)=0\,, \tag{4a}$$

whereas eq. (2b) does not change insofar the stresses do not depend on the displacements themselves but on their spatial gradients:

$$\tau_{xy}(x, y = H, t) = 0 \qquad \sigma_{yy}(x, y = H, t) = 0\,, \tag{4b}$$

similarly eq. (2b) becomes

$$\tau_{xy}(x = 0, y, t) = 0 \qquad u(x = 0, y, t) = 0\,. \tag{4c}$$

Note that the original problem can be classified as “unforced wave propagation with inhomogeneous mixed boundary conditions", while this modified one corresponds to “forced wave propagation (because now there is an external body force $\rho\ddot{\mathbb{X}}_g$ in eq. (3a) with homogeneous mixed boundary conditions".

Purposefully, nothing has been said about initial conditions since we shall focus on steady-state response to a harmonic load. Considering a transient regime governed by the initial conditions can be achieved by appealing to Laplace’s transform in time. This could be easily done, but it would entail extra muddling of the problem, as one would have to invert yet another integral transform.

2.3 Dealing with the time domain: assume harmonic loading and steady-state response

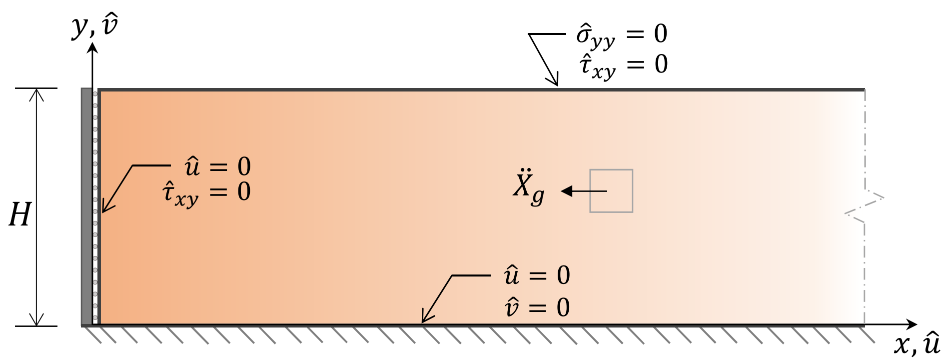

Figure 4: System after assuming harmonic excitation and response

The disclosed objective of this work is, chiefly, finding the transfer function for the earth thrust on the wall, therefore a more-convenient, equivalent way of proceeding is assuming a harmonic decomposition of both the load and the response and, invoking superposition, focus onto one sole harmonic. In summary, this means assuming $u = \hat{u}e^{i\varpi t}$, $v = \hat{v}e^{i\varpi t}$ as well as $\ddot{\mathbb{X}} = \ddot{X}_g e^{i\varpi t}$, where ϖ can be any excitation frequency and $\hat{u}$, $\hat{v}$ must be understood as complex numbers, whose modulus represents the magnitude of each displacement and its argument represents the phase lag between load and response. Introducing these changes into eq. (3) yields

$$(\lambda + 2\mu)\frac{\partial^2 \hat{u}}{\partial x^2} + (\lambda + \mu)\frac{\partial^2 v}{\partial x \partial y} + \mu\frac{\partial^2 \hat{u}}{\partial y^2} + \rho\varpi^2\hat{u} = \rho\ddot{X}_g(t)\,, \tag{5a}$$

$$(\lambda + 2\mu)\frac{\partial^2 \hat{v}}{\partial y^2} + (\lambda + \mu)\frac{\partial^2 \hat{u}}{\partial x \partial y} + \mu\frac{\partial^2 \hat{v}}{\partial x^2} + \rho\varpi^2\hat{v} = 0\,, \tag{5b}$$

with boundary conditions (from eqs. (4a) to (4c)):

$$\hat{u}(x, y = 0) = 0 \qquad \hat{v}(x, y = 0) = 0\,, \tag{6a}$$

$$\hat{\tau}_{xy}(x, y = H) = 0 \qquad \hat{\sigma}_{yy}(x, y = H) = 0\,, \tag{6b}$$

$$\hat{\tau}_{xy}(x = 0, y) = 0 \qquad \hat{u}(x = 0, y) = 0\,, \tag{6c}$$

2.4 Nondimensionalization and key symmetry argument

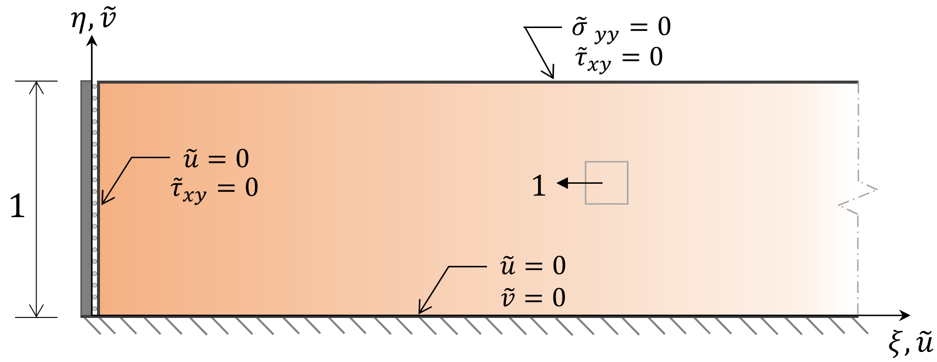

Figure 5: System after non-dimensionalization

Working with dimensionless equations makes easier to keep track of the parameters of the problem and eases the burden of algebraic manipulations. Regardless its convenience, this step is optional and does not bear any significance within the solving procedure. For the purpose of writing the last equations in dimensionless form, the following dimensionless variables and parameters are introduced:

$$\xi = x/H\,, \qquad \eta = y/H\,, \qquad \tilde{u} = \frac{\hat{u}}{\rho \ddot{X}_g H^2/\mu}\,, \qquad \tilde{v} = \frac{\hat{v}}{\rho \ddot{X}_g H^2/\mu}\,, \qquad r = \frac{\varpi}{c_s/H}\,, \qquad c = \sqrt{\frac{\lambda + 2\mu}{\mu}}\,, \tag{7a}$$

where ξ represents the dimensionless horizontal coordinate, η the dimensionless vertical coordinate, whereas $\tilde{u}$ and $\tilde{v}$ are the dimensionless horizontal and vertical displacement respectively, r is a dimensionless excitation frequency and $c = c(\nu) = c_s/c_p = \sqrt{(2(1-\nu))/(1-2\nu)}$ is the ratio between P-wave and S-wave propagation velocities which, in the case of isotropic linear-elastic solid, is a function of the Poisson's ratio, ν, solely.

Once again, use this change of variables to turn the equations of motion, eq. (5), into

$$c^2 \frac{\partial^2 \tilde{u}}{\partial \xi^2} + (c^2 - 1)\frac{\partial^2 \tilde{v}}{\partial \xi \eta} + \frac{\partial^2 \tilde{u}}{\partial \eta^2} + r^2 \tilde{u} = 1\,, \tag{8a}$$

$$c^2 \frac{\partial^2 \tilde{v}}{\partial \eta^2} + (c^2 - 1)\frac{\partial^2 \tilde{u}}{\partial \xi \eta} + \frac{\partial^2 \tilde{v}}{\partial \xi^2} + r^2 \tilde{v} = 0\,, \tag{8b}$$

subject to the boundary conditions, eqs. (6a) to (6c), at $\eta = 0$:

$$\tilde{u}(\xi, \eta = 0) = 0 \quad \tilde{v}(\xi, \eta = 0) = 0\,, \tag{9a}$$

at $\eta = 1$

$$\tau_{xy}(\xi, \eta = 1) = 0 \rightarrow \frac{\partial \tilde{u}}{\partial \eta}\Big|_{\eta=1} + \frac{\partial \tilde{v}}{\partial \xi}\Big|_{\eta=1} = 0\,, \tag{9b}$$

$$\sigma_{yy}(\xi, \eta = 1) = 0 \rightarrow c^2 \frac{\partial \tilde{v}}{\partial \eta}\Big|_{\eta=1} + (c^2 - 2)\frac{\partial \tilde{u}}{\partial \xi}\Big|_{\eta=1} = 0\,, \tag{9c}$$

at $\xi = 0$ (smooth, rigid wall)

$$\tilde{u}(\xi = 0, \eta) = 0\,, \tag{9d}$$

$$\tau_{xy}(\xi = 0, \eta) = 0 \rightarrow \frac{\partial \tilde{u}}{\partial \eta}\Big|_{\xi=0} + \frac{\partial \tilde{v}}{\partial \xi}\Big|_{\xi=0} = \frac{\partial \tilde{v}}{\partial \xi}\Big|_{\xi=0} = 0\,. \tag{9e}$$

At this moment one must consider how to deal with the unboundedness of the horizontal coordinate. Since $x \in [0, +\infty)$, an approach based on applying Laplace's transform on displacements may seem on point at first, however opting for this approach requires knowledge of both the value of the displacement and its first derivative at the wall, what is not the case: the value of $\tilde{u}$ is known yet $\partial \tilde{u}/\partial \xi$ is not, and conversely $\partial \tilde{v}/\partial \xi$ is known while $\tilde{v}$ is not. Thus, applying Laplace's transform would mean entering a cul-de-sac. Nevertheless, the conditions seem ideal to apply Fourier sine transform and Fourier cosine transform, yet this option appears confusing as it would require using different transforms for each displacement field component.

The fitting approach for this specific problem is appealing to symmetry and then applying the classic Fourier Transform. The symmetry argument reads: this type of one-wall system formulated in terms of relative displacements, amounts to applying a symmetry condition on a infinite layer wherein the body force suddenly changes sign, but not magnitude, at $\xi = 0$.

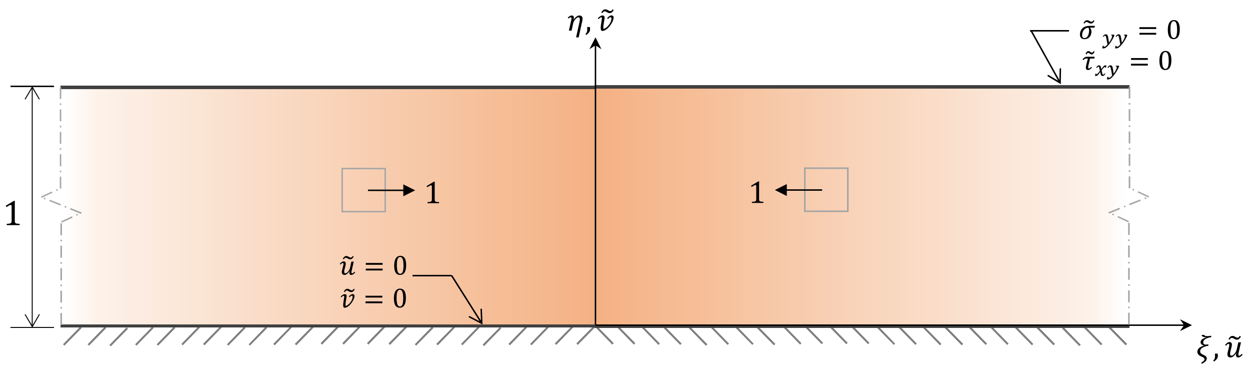

Figure 6: Nondimensional system after applying symmetry argument

Thus, in lieu of the semi-infinite soil strip domain, let us consider a infinite domain $\xi \in (-\infty, +\infty)$, where at $\xi = 0$ there is a discontinuity in the "loading", that is, the external body force, originally simply -1 defined over $x \geq 0$, now follows a step function, $1 - 2\theta(\xi)$ defined over $x \in \mathbb{R}$, where $\theta(\xi)$ is the Heaviside function centered at $\xi = 0$.

Hence, the system that will finally be solved is governed by the following equations and boundary conditions (equivalent to eq. (8) with boundary conditions (9)):

$$c^2 \frac{\partial^2 \tilde{u}}{\partial \xi^2} + (c^2 - 1)\frac{\partial^2 \tilde{v}}{\partial \xi \eta} + \frac{\partial^2 \tilde{u}}{\partial \eta^2} + r^2 \tilde{u} = 2\theta(\xi) - 1\,, \tag{10a}$$

$$c^2 \frac{\partial^2 \tilde{v}}{\partial \eta^2} + (c^2 - 1)\frac{\partial^2 \tilde{u}}{\partial \xi \eta} + \frac{\partial^2 \tilde{v}}{\partial \xi^2} + r^2 \tilde{v} = 0\,, \tag{10b}$$

subject to the boundary conditions at $\eta = 0$:

$$\tilde{u}(\xi, \eta = 0) = 0 \quad \tilde{v}(\xi, \eta = 0) = 0\,, \tag{11a}$$

at $\eta = 1$

$$\tau_{xy}(\xi, \eta = 1) = 0 \rightarrow \left.\frac{\partial \tilde{u}}{\partial \eta}\right|_{\eta=1} + \left.\frac{\partial \tilde{v}}{\partial \xi}\right|_{\eta=1} = 0\,, \tag{11b}$$

$$\sigma_{yy}(\xi, \eta = 1) = 0 \rightarrow c^2 \left.\frac{\partial \tilde{v}}{\partial \eta}\right|_{\eta=1} + (c^2 - 2)\left.\frac{\partial \tilde{u}}{\partial \xi}\right|_{\eta=1} = 0\,. \tag{11c}$$

Resorting to Fourier Transform [Weinberger, 2012]:

$$F[\tilde{u}] = \frac{1}{\sqrt{2\pi}} \int_{-\infty}^{+\infty} \tilde{u} e^{ik\xi} d\xi = U\,, \tag{12a}$$

$$F[\tilde{v}] = \frac{1}{\sqrt{2\pi}} \int_{-\infty}^{+\infty} \tilde{v} e^{ik\xi} d\xi = V\,, \tag{12b}$$

where k is the dimensionless wavenumber (its relation to the physical wavenumber k being $\mathrm{k}H = k$), hence eq. (10) becomes

$$ik(c^2 - 1)\frac{\partial V}{\partial \eta} + \frac{\partial^2 U}{\partial \eta^2} + (r^2 - c^2 k^2)U - \sqrt{\frac{2}{\pi}}\frac{i}{k} = 0\,, \tag{13a}$$

$$c^2 \frac{\partial^2 V}{\partial \eta^2} + ik(c^2 - 1)\frac{\partial U}{\partial \eta} + (r^2 - k^2)V = 0\,, \tag{13b}$$

likewise, eq. (11) becomes the following: at $\eta = 0$

$$U(0) = 0 \quad V(0) = 0\,, \tag{14a}$$

at $\eta = 1$

$$\tau_{xy} = 0 \rightarrow \left.\frac{\partial U}{\partial \eta}\right|_{\eta=1} + ikV = 0\,, \tag{14b}$$

$$\sigma_{yy} = 0 \rightarrow c^2 \left.\frac{\partial V}{\partial \eta}\right|_{\eta=1} + ik(c^2-2)U = 0\,, \tag{14c}$$

what represents the problem in the original vertical (nondimensional) variable and in wavenumber (k) domain, assuming harmonic loading and steady-state conditions.

2.5 Reaching the solution in horizontal wavenumber space

The system of equations (13) can be even more condensed by introducing extra auxiliary variables $\mathcal{V} = \partial V/\partial \eta$, $\mathcal{U} = \partial U/\partial \eta = \partial[U - (k(r^2 - c^2k^2))^{-1}]/\partial \eta$:

$$\frac{\partial \mathcal{U}}{\partial \eta} = ik(1-c^2)\mathcal{V} + (c^2k^2 - r^2)\left(U + \sqrt{\frac{2}{\pi}}\frac{i}{k(c^2k^2-r^2)}\right)\,, \tag{15a}$$

$$\frac{\partial}{\partial \eta}\left(U + \sqrt{\frac{2}{\pi}}\frac{i}{k(c^2k^2-r^2)}\right) = \mathcal{U}\,, \tag{15b}$$

$$\frac{\partial \mathcal{V}}{\partial \eta} = ik\frac{(1-c^2)}{c^2}\mathcal{U} + \frac{(k^2-r^2)}{c^2}V\,, \tag{15c}$$

$$\frac{\partial V}{\partial \eta} = \mathcal{V}\,, \tag{15d}$$

subject to the boundary conditions equivalent to (14): at $\eta = 0$

$$U(0) = 0 \quad V(0) = 0\,, \tag{16a}$$

at $\eta = 1$

$$\mathcal{U}(1) = -ikV(1)\,, \tag{16b}$$

$$c^2\mathcal{V}(1) = -ik(c^2-2)U(1)\,. \tag{16c}$$

Introducing a vector of unknowns, $\boldsymbol{X} = \begin{bmatrix} \mathcal{U} & U + \sqrt{\frac{2}{\pi}}\frac{i}{k(c^2k^2-r^2)} & \mathcal{V} & V \end{bmatrix}^T$, eq. (15) can be written simply as

$$\boldsymbol{X}' = \boldsymbol{D}\boldsymbol{X}\,, \tag{17}$$

where

$$\boldsymbol{D} = \begin{bmatrix} 0 & (c^2k^2-r^2) & ik(1-c^2) & 0 \\ 1 & 0 & 0 & 0 \\ ik\frac{(1-c^2)}{c^2} & 0 & 0 & \frac{(k^2-r^2)}{c^2} \\ 0 & 0 & 1 & 0 \end{bmatrix}\,. \tag{18}$$

The eigenvalues of this matrix are

$$\lambda_1 = -\sqrt{k^2-r^2}\,, \quad \lambda_2 = \sqrt{k^2-r^2}\,, \quad \lambda_3 = -\sqrt{k^2-(r/c)^2}\,, \quad \lambda_4 = \sqrt{k^2-(r/c)^2}\,, \tag{19}$$

each of these solution corresponds to S-waves (first two solutions) and P-waves (last two solutions) propagating within this infinite stratum.

The eigenvectors (normalized to 1 in the fourth entry) are

$$\boldsymbol{\varphi}_1 = \begin{bmatrix} i\frac{(k^2-r^2)}{k} \\ -i\frac{(\sqrt{k^2-r^2})}{k} \\ -\sqrt{k^2-r^2} \\ 1 \end{bmatrix}\,, \quad \boldsymbol{\varphi}_2 = \begin{bmatrix} i\frac{(k^2-r^2)}{k} \\ i\frac{(\sqrt{k^2-r^2})}{k} \\ \sqrt{k^2-r^2} \\ 1 \end{bmatrix}\,, \quad \boldsymbol{\varphi}_3 = \begin{bmatrix} ik \\ -i\frac{k}{\sqrt{k^2-(r/c)^2}} \\ -\sqrt{k^2-(r/c)^2} \\ 1 \end{bmatrix}\,, \quad \boldsymbol{\varphi}_4 = \begin{bmatrix} ik \\ i\frac{k}{\sqrt{k^2-(r/c)^2}} \\ \sqrt{k^2-(r/c)^2} \\ 1 \end{bmatrix}\,, \tag{20}$$

thus the solution must be

$$\boldsymbol{X} = \begin{bmatrix} \mathcal{U} \\ U + \sqrt{\frac{2}{\pi}}\frac{i}{k(c^2k^2-r^2)} \\ \mathcal{V} \\ V \end{bmatrix} = A \begin{bmatrix} i\frac{(k^2-r^2)}{k} \\ -i\frac{(\sqrt{k^2-r^2})}{k} \\ -\sqrt{k^2-r^2} \\ 1 \end{bmatrix} e^{-\sqrt{k^2-r^2}\eta} + B \begin{bmatrix} i\frac{(k^2-r^2)}{k} \\ i\frac{(\sqrt{k^2-r^2})}{k} \\ \sqrt{k^2-r^2} \\ 1 \end{bmatrix} e^{\sqrt{k^2-r^2}\eta}$$
$$+C \begin{bmatrix} ik \\ -i\frac{k}{\sqrt{k^2-(r/c)^2}} \\ -\sqrt{k^2-(r/c)^2} \\ 1 \end{bmatrix} e^{-\sqrt{k^2-(r/c)^2}\eta} + D \begin{bmatrix} ik \\ i\frac{k}{\sqrt{k^2-(r/c)^2}} \\ \sqrt{k^2-(r/c)^2} \\ 1 \end{bmatrix} e^{\sqrt{k^2-(r/c)^2}\eta}, \tag{21}$$

or introducing the following shorthands $\alpha = \sqrt{k^2-r^2}$, $\beta = \sqrt{k^2-(r/c)^2}$:

$$\boldsymbol{X} = \begin{bmatrix} \mathcal{U} \\ U + \sqrt{\frac{2}{\pi}}\frac{i}{c^2k\beta^2} \\ \mathcal{V} \\ V \end{bmatrix} = A \begin{bmatrix} i\frac{\alpha^2}{k} \\ -i\frac{\alpha}{k} \\ -\alpha \\ 1 \end{bmatrix} e^{-\alpha\eta} + B \begin{bmatrix} i\frac{\alpha^2}{k} \\ i\frac{\alpha}{k} \\ \alpha \\ 1 \end{bmatrix} e^{\alpha\eta} + C \begin{bmatrix} ik \\ -i\frac{k}{\beta} \\ -\beta \\ 1 \end{bmatrix} e^{-\beta\eta} + D \begin{bmatrix} ik \\ i\frac{k}{\beta} \\ \beta \\ 1 \end{bmatrix} e^{\beta\eta}, \tag{22}$$

where A, B, C, D are "constants" (which nevertheless depend on the parameter k) to be determined from the boundary conditions, starting from the easiest ones, $V(0) = 0$ and $U(0) = 0$

$$V(0) = A + B + C + D = 0, \tag{23}$$

$$U(0) = \frac{i\alpha}{k}(B-A) + \frac{ik}{\beta}(D-C) - \sqrt{\frac{2}{\pi}}\frac{i}{c^2k\beta^2} = 0, \tag{24}$$

followed by the most convoluted conditions at $\eta = 1$, $\tau_{xy} = 0$

$$\mathcal{U}(1) + ikV(1) = 0 \rightarrow \frac{i\alpha^2}{k}(Ae^{-\alpha} + Be^{\alpha}) + ik(Ce^{-\beta} + De^{\beta}) = 0, \tag{25a}$$

$$ik(Ae^{-\alpha} + Be^{\alpha}) + ik(Ce^{-\beta} + De^{\beta}) = 0, \tag{25b}$$

$$\left(k + \frac{\alpha^2}{k}\right)(Ae^{-\alpha} + Be^{\alpha}) + 2k(Ce^{-\beta} + De^{\beta}) = 0, \tag{25c}$$

and $\sigma_{yy} = 0$

$$c^2\mathcal{V}(1) + ik(c^2-2)\left(U(1) \pm \sqrt{\frac{2}{\pi}}\frac{i}{c^2k\beta^2}\right) = 0, \tag{26a}$$

$$\begin{aligned} &c^2\mathcal{V}(1) + ik(c^2-2)\left(U(1) + \sqrt{\frac{2}{\pi}}\frac{i}{c^2k\beta^2}\right) = -\sqrt{\frac{2}{\pi}}\frac{(c^2-2)}{c^2\beta^2} = \\ &= c^2\alpha(Be^{\alpha} - Ae^{-\alpha}) + c^2\beta(De^{\beta} - Ce^{-\beta}) \\ &- (c^2-2)\alpha(Be^{\alpha} - Ae^{-\alpha}) - (c^2-2)\frac{k^2}{\beta}(De^{\beta} - Ce^{-\beta}) \\ &= 2\alpha(Be^{\alpha} - Ae^{-\alpha}) + \left(\frac{c^2(\beta^2-k^2)+2k^2}{\beta}\right)(De^{\beta} - Ce^{-\beta}). \end{aligned} \tag{26b}$$

Recast eqs. (23), (24), (25c) and (26b) in matrix form:

$$\begin{bmatrix} 1 & 1 & 1 & 1 \\ -\frac{i\alpha}{k} & \frac{i\alpha}{k} & -\frac{ik}{\beta} & \frac{ik}{\beta} \\ \left(k + \frac{\alpha^2}{k}\right)e^{-\alpha} & \left(k + \frac{\alpha^2}{k}\right)e^{\alpha} & 2ke^{-\beta} & 2ke^{\beta} \\ -2\alpha e^{-\alpha} & 2\alpha e^{\alpha} & -\left(\frac{c^2(\beta^2-k^2)+2k^2}{\beta}\right)e^{-\beta} & \left(\frac{c^2(\beta^2-k^2)+2k^2}{\beta}\right)e^{\beta} \end{bmatrix} \begin{bmatrix} A \\ B \\ C \\ D \end{bmatrix} = \begin{bmatrix} 0 \\ \sqrt{\frac{2}{\pi}}\frac{i}{c^2k\beta^2} \\ 0 \\ -\sqrt{\frac{2}{\pi}}\frac{(c^2-2)}{c^2\beta^2} \end{bmatrix}, \tag{27}$$

the value of the constants is found after solving (inverting) this linear system. The actual expressions are computed by recourse to *Mathematica* [Wolfram, 2000]. The expressions are frankly convoluted, and so long that cannot fit in one landscape page.

There is no direct formula to invert the integrals where the coefficients appear. Analytical inversions must be performed by recourse to Contour Integration and Residue Calculus [Lang, 2013], what turns out to be an extensive and challenging task the author has not succeeded in carrying out yet.

3 Evaluating and verifying the solution

Instead of taking that path, one can try to approximate the integral numerically, as the coefficients can be easily obtained in *Mathematica*.

In order to approximate this integral numerically the integration has to be stopped at some point; it is known (from previous study carried out by the author in the context of his doctoral thesis [Garcia-Suarez, 2019]) that the horizontal wavelengths $\sim H$ are those that control the response close to the wall (and these are the shortest wavelength that are present), therefore limiting the integration to $|k| \in [0, 10]$ guarantees all these are all accounted.

Once these coefficients have been computed, the solution in wavenumber domain has been found. Results derived from the exact solution are going to be compared to FEM analysis performed on *Abaqus* [Simulia, 2010]. This package, at the time the simulations were run, does not contain elements suitable to model *open boundaries* [Esmaeilzadeh Seylabi, 2016]. For this reason, as the unboundedness in the horizontal direction can not be accounted formally, a very slender model ($H/L = 100$, L being the horizontal length of the part) was used. This approach mirrors the one advocated recently by Durante and collaborators [Durante et al., 2018], which delivered satisfactory results in the quasi-static regime, yet it had not been tested in frequency-domain dynamic analysis previously.

The parameter models are encapsulated in the following table. Keep in mind that *Abaqus* does not require to input units, and the user is solely responsible for ensuring the use of a consistent set of units.

Young's modulus E (GPa)	Density ρ (kg/m^3)	Height H (m)	Acceleration $\ddot{X}_g$ (m/s^2)
10	2000	2	0.73

Table 1: Physical parameters used in finite-element simulations

3.1 Vertical displacement at upper-left corner

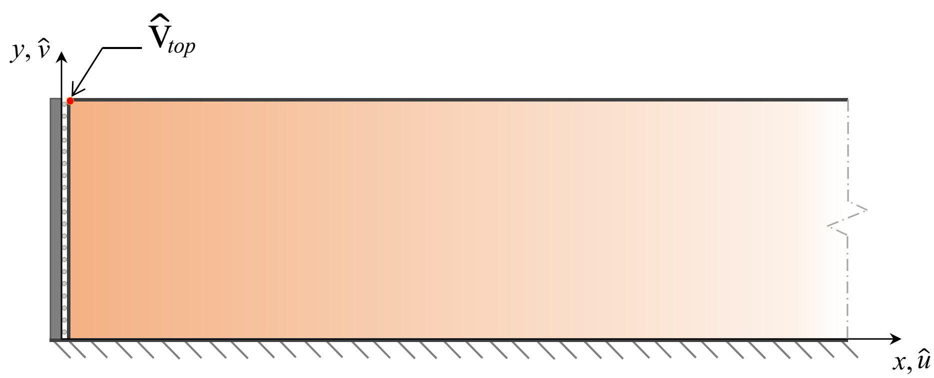

Figure 7: Probe location for $\tilde{\text{v}}_{top}$

One can then move to calculate, for instance, the vertical displacement at the top of the wall, $\tilde{v}(\eta = 1, \xi = 0) = \tilde{\text{v}}_{top}$, by inverting the transform:

$$\tilde{\text{v}}_{top} = F^{-1}[V]_{\eta=1,\xi=0} = \frac{1}{\sqrt{2\pi}} \int_{-\infty}^{+\infty} \left[V e^{-ik\xi}\right]_{\eta=1,\xi=0} dk \,, \tag{28a}$$

recall $V = Ae^{-\alpha\eta} + Be^{\alpha\eta} + Ce^{-\beta\eta} + De^{\beta\eta}$,

$$= \frac{1}{\sqrt{2\pi}} \int_{-\infty}^{+\infty} \left[Ae^{-\alpha} + Be^{\alpha} + Ce^{-\beta} + De^{\beta}\right] dk \,, \tag{28b}$$

where, bear in mind, A, B, C, D, α, and β are functions of the dimensionless wavenumber k, and the integration is limited to $k \in [-10, 10]$.

The comparison of eq. (28b), as evaluated in *Mathematica*, to the results obtained in *Abaqus*, once properly expressed in non-dimensional form, is displayed in Figures 8 and 9. The first plot corresponds to $\delta_d = 0.05$ and the second one to $\delta_d = 0.16$, and in both bases $\nu = 0.1$ and $r = \pi\varpi/2\omega_s \in [0, 5\pi/4]$, $\omega_s = \pi c_s/2H$.

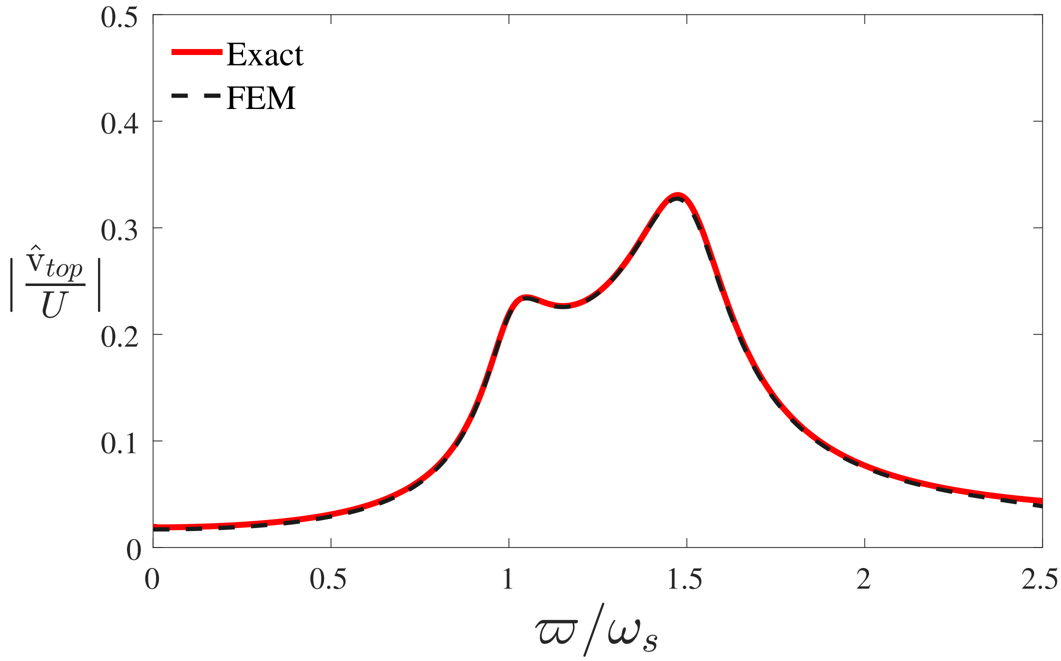

Figure 8: Transfer function for the vertical displacement at the top of the wall, $\nu = 0.1$, $\delta_d = 0.16$

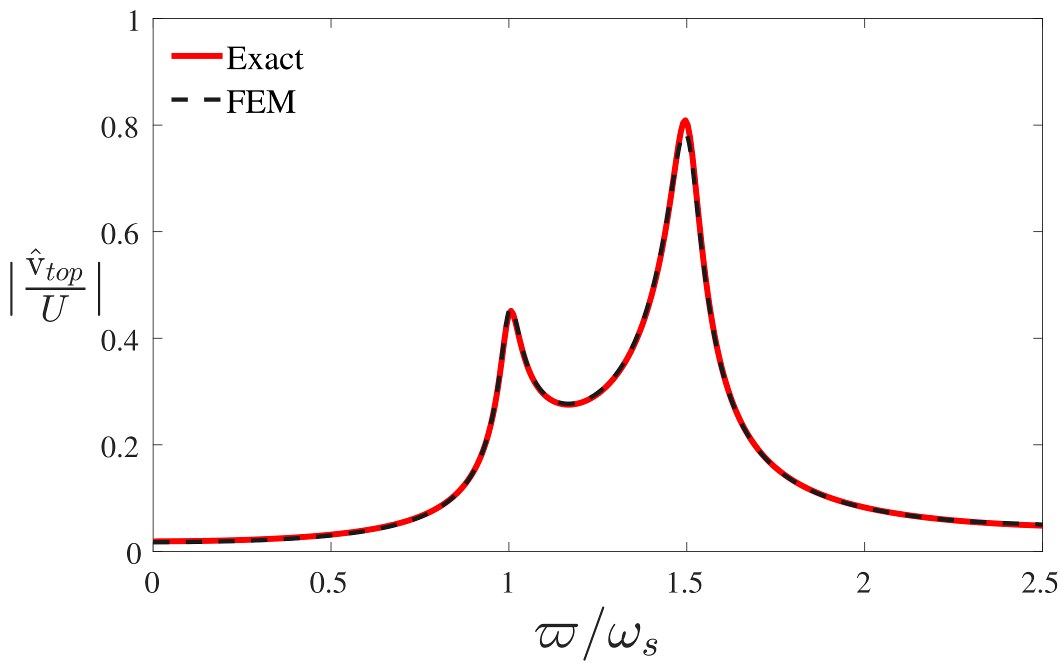

Figure 9: Transfer function for the vertical displacement at the top of the wall, $\nu = 0.1$, $\delta_d = 0.05$

Full agreement is acknowledged in both Figure 8 and Figure 9. It must be highlighted that, for $\nu = 0.1$ we observe a second resonance, that would not be present in the far-field response, at $\varpi \approx 1.5\omega_s = c\,\omega_s = \omega_p$, since $c = c_p/c_s = 1.5$ when $\nu = 0.1$.

3.2 Earth thrust over the wall

The earth thrust represents the integral of the stresses that develop at the soil-wall interface. In the case of the smooth wall, harmonic loading and steady-state conditions, it can be written as

$$Q = \hat{Q} e^{i\varpi t} = e^{i\varpi t} \int_0^H \hat{\sigma}_{xx}(x=0,y)\, dy\,, \tag{29}$$

ergo the amplitude of the thrust can be expressed in terms of the solution coefficients in horizontal wavenumber domain as the next inverse Fourier transform:

$$\frac{\hat{Q}}{\rho \ddot{X}_g H^2} = \frac{1}{\sqrt{2\pi}} \int_{-\infty}^{+\infty} \left\{ \frac{\sqrt{2/\pi}}{\beta^2} + c^2(A+B) - 2(Ae^{-\alpha} + Be^{\alpha}) + \right. \\ \left. + \left[c^2 \left(1 - \left(\frac{k}{\beta} \right)^2 \right) - 2 \right] \left(Ce^{-\beta} + De^{\beta} \right) + \left(\frac{ck}{\beta} \right)^2 (C+D) \right\} dk\,. \tag{30}$$

Similarly to eq. (28b), the equation can be evaluated numerically. For $\nu = 1/3$ and $\delta_d = 0.01$, see Figure 10.

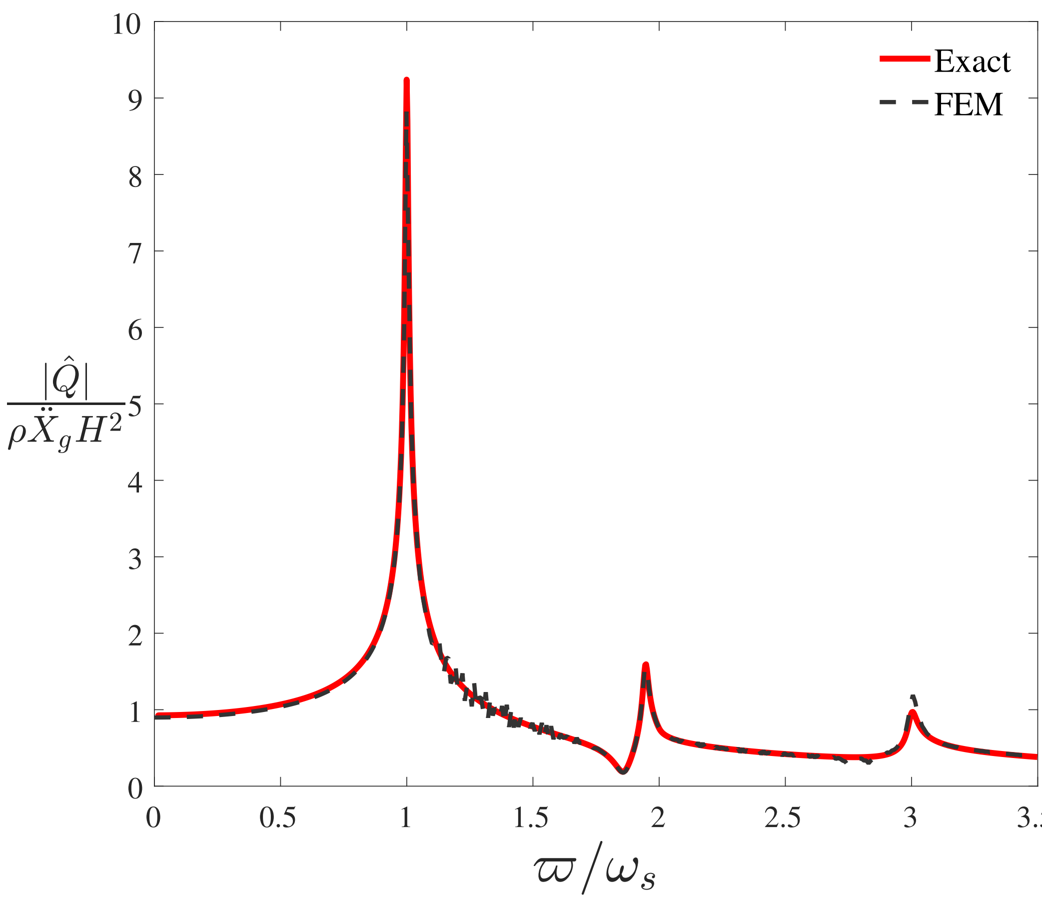

Figure 10: Transfer function for the earth thrust the wall, $\nu = 1/3$, $\delta_d = 0.01$

Let us spend a moment commenting Figure 10. There seems to be some numerical artifact the author has not yet identified, which makes the numerical result oscillate mildly between the first two spikes. Other than that, the agreement is complete. All the features predicted by the exact solution are present in the FEM analysis, including a substantive "dip" (deamplification) right before the second peak. As reported in Figure 8 and following ones,this resonance happens at $\varpi \approx 2\omega_s = c\,\omega_s = \omega_p$, since $c_p/c_s = 2$ as $\nu = 1/3$. This secondary resonance would have been overlooked had we assumed the thrust resonates at the same natural frequencies as the 1D soil column in the far-field [Veletsos and Younan, 1994a].

The effect of damping on the thrust is addressed in Figure 11. The figures correspond to $\nu = 0.1$ (so one should expect, again, to find resonance at $\varpi/\omega_s = 1, 1.5, 3$ and so on), three different increasing values of damping are used $\delta_d = 0.05, 0.1, 0.2,$, and, again, $r = \pi\varpi/2\omega_s \in [0\,, 7\pi/4]$.

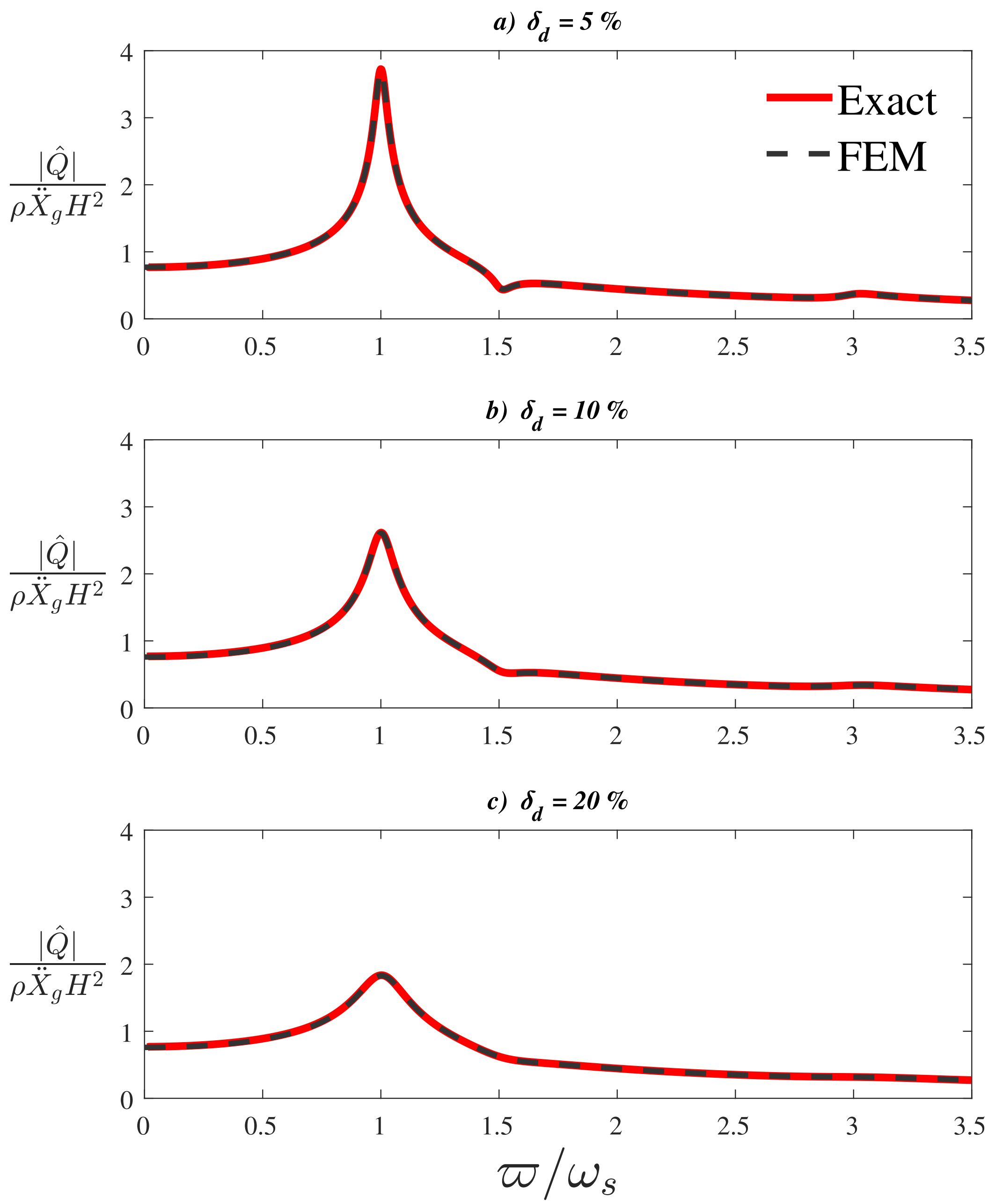

Figure 11: Transfer function for the earth thrust the wall, $\nu = 0.1$, $\delta_d = 0.05, 0.1, 0.2$

Once again, there is total compliance of numerical to analytical results, in the three cases. It is instructive to note how increasing damping scratches out the two second resonant peaks and the aforesaid dip that happens before the resonance associated to ω_p. This secondary resonance origin has not been fully figured out yet: it remains to explain if it is an artifact of mode conversion or of a surface wave propagating along the wall-soil interface, and how pernicious its effects can be over the wall integrity. A certain aspect is clear: it had been unaccounted for in the previous engineering solutions, which displayes resonance at the wall at the same natural frequencies as the far-field.

4 Conclusions and future work

This document shows that the Younan-Veletsos problem admits an exact steady-state solution that can be expressed by means of elementary functions in horizontal wavenunber space, and details a formal procedure to obatin it. By evaluating the solution numerically, it has been shown that there exist resonance phenomena that current simplified models do not capture, as the latter presuppose that the natural frequencies of the displacement field close to the wall resemble those of the displacement at the far-field.

To formally close the problem, the inverse Fourier transform involving the coefficients in eq. (15) should be computed as to obtain the exact displacement field in every point of the domain.

This exact solution of the Younan-Veletsos problem can potentially be generalized to the case of *rough* wall (the soil being rigidly connected to the wall), by mildly tweaking the boundary conditions at the wall and applying the same procedure outlined in this text; another interesting extension is the *flexible* wall case, what would provide new insight on the relation between wall stiffness and seismic earth pressures so as to confirm the insight obtained by Veletsos and Younan through simplified models and simulations [Younan and Veletsos, 2000].

5 Acknowledgments

The format used in this preprint has been dispensed by Mr. George Kour through *Overleaf* under Creative Commons CC BY 4.0.

6 Supplementary material

This paper contains results from the first author's thesis [Garcia-Suarez, 2019]. A Mathematica notebook titled *Chapter4 Exact Solution YV Problem.nb*, containing the actual expression of the coefficients (A, B, C, D) in eq. (27) and evaluation of the functions leading to the plots that are displayed in this text, can be found in the first author's GitHub (`github.com/jgarciasuarez`, repository name: `thesis_mathematica-`).
References in the markdowns in the notebook are linked to the text of the thesis, not to the one of this preprint.

References

[Barends, 1980] Barends, F. (1980). Dynamics of elastic plates on a flexible subsoil. *LGM-Mededelingen*, 21:127–134.

[Brandenberg et al., 2015] Brandenberg, S. J., Mylonakis, G., and Stewart, J. P. (2015). Kinematic framework for evaluating seismic earth pressures on retaining walls. *Journal of Geotechnical and Geoenvironmental Engineering*, 141(7):04015031.

[Building Seismic Safety Council, 2009] Building Seismic Safety Council, B. (2009). Nehrp recommended seismic provisions for new buildings and other structures (fema p-750).

[Candia et al., 2016] Candia, G., Mikola, R. G., and Sitar, N. (2016). Seismic response of retaining walls with cohesive backfill: Centrifuge model studies. *Soil Dynamics and Earthquake Engineering*, 90:411–419.

[Coulomb, 1973] Coulomb, C. A. (1973). Essai sur une application des regles de maximis et minimis a quelques problemes de statique relatifs a l'architecture (essay on maximums and minimums of rules to some static problems relating to architecture).

[Durante et al., 2018] Durante, M. G., Brandenberg, S. J., Stewart, J. P., and Mylonakis, G. (2018). *Winkler Stiffness Intensity for Flexible Walls Retaining Inhomogeneous Soil*.

[Esmaeilzadeh Seylabi, 2016] Esmaeilzadeh Seylabi, E. (2016). *Reduced order modeling of soil structure interaction problems*. PhD thesis, UCLA.

[Garcia-Suarez, 2019] Garcia-Suarez, J. (2019). *Application of path-independent integrals to soil-structure interaction*. PhD thesis, California Institute of Technology.

[Keykhosropour and Lemnitzer, 2019] Keykhosropour, L. and Lemnitzer, A. (2019). Experimental studies of seismic soil pressures on vertical flexible, underground structures and analytical comparisons. *Soil Dynamics and Earthquake Engineering*, 118:166–178.

[Kloukinas et al., 2012] Kloukinas, P., Langousis, M., and Mylonakis, G. (2012). Simple wave solution for seismic earth pressures on non-yielding walls. 138:1514–1519.

[Lang, 2013] Lang, S. (2013). *Complex analysis*, volume 103. Springer Science & Business Media.

[Love, 2013] Love, A. E. H. (2013). *A treatise on the mathematical theory of elasticity*. Cambridge university press.

[Lubliner, 2008] Lubliner, J. (2008). *Plasticity theory*. Courier Corporation.

[Matsuo and Ohara, 1960] Matsuo, H. and Ohara, S. (1960). Lateral earth pressure and stability of quay walls during earthquakes. In *Proceedings of the Second World Conference on Earthquake Engineering*, volume 1, pages 165–181. Science Council of Japan Tokyo-Kyoto, Japan.

[Miklowitz, 2012] Miklowitz, J. (2012). *The theory of elastic waves and waveguides*, volume 22. Elsevier.

[Mylonakis et al., 2007] Mylonakis, G., Kloukinas, P., and Papantonopoulos, C. (2007). An alternative to the mononobe–okabe equations for seismic earth pressures. *Soil Dynamics and Earthquake Engineering*, 27(10):957–969.

[Okabe, 1924] Okabe, S. (1924). General theory on earth pressure and seismic stability of retaining wall and dam. *J. of the Japan Society of Civil Engrg*, 10(6):1277–1323.

[Scott, 1973] Scott, R. (1973). Earthquake-induced pressures on retaining walls. In *Proceedings of the 5th World Conference on Earthquake Engineering*, volume 2, pages 1611–1620.

[Seed, 1970] Seed, H. (1970). Design of earth retaining structures for dynamic loads. In *ASCE Specialty Conf.-Lateral Stress in the Ground and Design of Earth Retaining Structures, 1970*.

[Simulia, 2010] Simulia, D. S. (2010). Abaqus analysis user's manual. *Dassault Systemes, Pawtucket, USA*.

[Steedman and Zeng, 1990] Steedman, R. and Zeng, X. (1990). The influence of phase on the calculation of pseudo-static earth pressure on a retaining wall. *Geotechnique*, 40(1):103–112.

[Veletsos and Younan, 1994a] Veletsos, A. and Younan, A. (1994a). Dynamic soil pressures on rigid vertical walls. *Earthquake engineering & structural dynamics*, 23(3):275–301.

[Veletsos and Younan, 1994b] Veletsos, A. S. and Younan, A. H. (1994b). Dynamic modeling and response of soil-wall systems. *Journal of Geotechnical Engineering*, 120(12):2155–2179.

[Verruijt, 1996] Verruijt, A. (1996). *Soil dynamics*. Technische Universiteit, Faculteit Civiele Techniek.

[Weinberger, 2012] Weinberger, H. F. (2012). *A first course in partial differential equations: with complex variables and transform methods*. Courier Corporation.

[Westergaard, 1938] Westergaard, H. (1938). A problem of elasticity suggested by a problem in soil mechanics: soft material reinforced by numerous strong horizontal sheets. *Contributions to the mechanics of solids, Stephen Timoshenko 60th anniversary volume*, pages 268–277.

[Wolfram, 2000] Wolfram, S. (2000). *The mathematica book*, volume 4. Cambridge University Press Cambridge.

[Wood, 1973] Wood, J. H. (1973). Earthquake-induced soil pressures on structures.

[Younan and Veletsos, 2000] Younan, A. and Veletsos, A. S. (2000). Dynamic response of flexible retaining walls. *Earthquake engineering & structural dynamics*, 29(12):1815–1844.